

HELIOSEISMOLOGY WITH LONG RANGE DARK MATTER-BARYON INTERACTIONS

LÍDIO LOPES^{1,2,7}, PAOLO PANCI^{3,4,7}, JOSEPH SILK^{4,5,6,7}

(Dated: December 3, 2024)
Draft version December 3, 2024

ABSTRACT

Assuming the existence of a primordial asymmetry in the dark sector, we study how DM-baryon long-range interactions, induced by the kinetic mixing of a new $U(1)$ gauge boson and the photon, affects the evolution of the Sun and in turn the sound speed profile obtained from helioseismology. Thanks to the explicit dependence on the exchanged momenta in the differential cross section (Rutherford-like scattering), we find that dark matter particles with a mass of ~ 10 GeV, kinetic mixing parameter in the range $10^{-10} - 10^{-9}$ and a mediator with a mass smaller than a few MeV improve the agreement between the best solar model and the helioseismic data without being excluded by direct detection experiments. In particular, the LUX detector will soon be able to either constrain or confirm our best fit solar model in the presence of a dark sector with long-range interactions that reconcile helioseismology with thermal neutrino results.

Keywords: cosmology: miscellaneous, dark matter, elementary particles, Sun: helioseismology

1. INTRODUCTION

The standard Λ CDM cosmological model has been successfully applied to explain the main characteristics of the Universe (see e.g. [Hinshaw et al. 2013](#); [Ade et al. 2013](#)). In particular, numerical simulations of collisionless cold Dark Matter (DM) describe the gravitational growth of infinitesimal primordial density perturbations, probed by the cosmic microwave background anisotropies, that lead to the formation of the present-day large-scale structure of the universe. These simulations provide us with a number of predictions about the structure of cold DM halos and their basic properties (see e.g. [Guo et al. 2013](#)). Although the standard cosmological model has proven to be highly successful in explaining the observed large-scale structure of the universe, it has been less successful on smaller scales. Recent data on low mass galaxies suggests that the inferred subhalo DM distributions have almost flat cores (see e.g. [de Blok 2010](#)), in contradiction with the cuspy profile distributions predicted by numerical simulations (see e.g. [Navarro et al. 2010](#)), and that sub halo numbers are overpredicted at both low mass and intermediate masses (see e.g. [Klypin et al. 1999](#)) and massive dwarf galaxy scales (see e.g. [Garrison-Kimmel et al. 2013](#)). Some of the issues associated with dwarf galaxies can be addressed if the DM is more "collisional" (with baryons) than currently considered in numerical simulations. For example, this

hypothesis favors constant-density cores with much lower central densities than those coming from the usual cold DM (see e.g. [Rocha et al. 2013](#)).

In addition, the closeness between Ω_{DM} and Ω_{b} , usually referred as cosmic coincidence, may suggest a profound link between the dark and the ordinary sectors. Indeed, although the two sectors have different macroscopic properties, the total amount of DM observed today could be produced in the early universe by a mechanism identical to baryogenesis, and therefore an asymmetry between DM particles and their antiparticles would be expected. A detailed account of current progress in asymmetric DM studies can be found in the literature (see e.g., [Petraki & Volkas 2013](#)).

All of these cosmological facts may suggest that dark and ordinary matter may have more properties in common than expected. In view of this, it is tantalizing to imagine that the dark world could be similarly complex (CP violating and asymmetric) and full of forces that are invisible to us (hidden parallel sector or mirror world⁸). The history of the early mirror universe has been studied in ref. ([Berezhiani et al. 2001](#)), while the impact of an hidden mirror sector in the CMB and LSS data can be found in ref. ([Berezhiani et al. 2005](#)). For a general review on the properties of a hidden world neighboring our own, see e.g. refs. ([Foot 2004b](#); [Berezhiani 2005](#)).

More specifically, since in our sector only long-range electromagnetic force and gravity affect the dynamical evolution of virialized astrophysical objects, the physics of a complex dark sector in which the matter fields are charged under an extra $U(1)$ gauge group is particularly interesting to study. Indeed, if the mass of the new gauge boson (dark photon) is smaller than the typical momenta exchanged in the scattering, the phenomenology of the dark world can in itself be as complicated as

⁸ The idea of a mirror world was suggested prior to the advent of the Standard Model (see e.g. Refs. ([Lee & Yang 1956](#); [Kobzarev et al. 1966](#)). The idea that the mirror particles might instead constitute the DM of the Universe was discussed in refs. ([Blinnikov & Khlopov 1982, 1983](#)).

¹ Centro Multidisciplinar de Astrofísica, Instituto Superior Técnico, Universidade Tecnica de Lisboa, Av. Rovisco Pais, 1049-001 Lisboa, Portugal

² Departamento de Física, Escola de Ciencia e Tecnologia, Universidade de Évora, Colégio Luis António Verney, 7002-554 Évora - Portugal

³ CP3-Origins and DIAS, University of Southern Denmark, Odense, Denmark

⁴ Institut d'Astrophysique, UMR 7095 CNRS, Université Pierre et Marie Curie, 98bis Blvd Arago, 75014 Paris, France

⁵ Department of Physics and Astronomy, The Johns Hopkins University, Baltimore, MD21218

⁶ Beecroft Institute for Cosmology and Particle Astrophysics, University of Oxford, Keble Road, Oxford OX1 3RH, UK

⁷ E-mails: (IL) ilidio.lobes@tecnico.ulisboa.pt; (PP) panci@iap.fr; (JS) silk@astro.ox.ac.uk

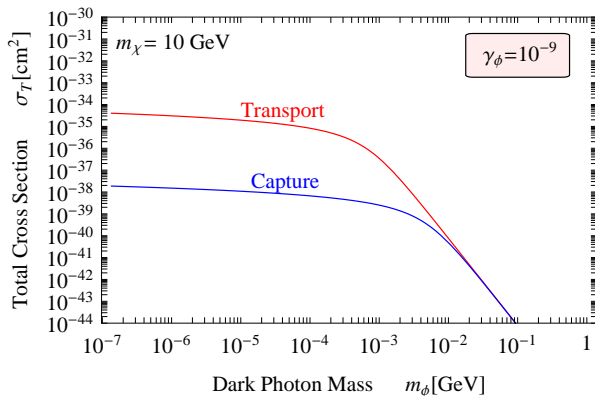


Figure 1. An illustrative example of the DM-hydrogen energy transfer cross section as a function of the mass of the dark photon m_ϕ for a fix value of the kinetic mixing parameter $\gamma_\phi = 10^{-9}$ and a DM mass $m_\chi = 10$ GeV. In blue is shown the scattering cross section responsible for the capture process σ_T^{cap} , while in red the one entering in the energy transport mechanism σ_T^{tra} computed at the present time ($T_c^0 = 1.57 \times 10^7$ K).

that of our sector (e.g. dark electromagnetism with quite large self-interactions), providing at the same time also a feeble long-range interaction between the two worlds (thanks to the kinetic mixing of the new $U(1)$ gauge boson with the photon). This implies in general that the dark world is more collisional than the standard cold DM, and therefore some of the previously mentioned problems can probably be solved (see e.g. [Loeb & Weiner 2011](#)).

In addition, since a long-range DM-nucleus interaction is enhanced for small momentum exchanges, this class of models can also relax the tension between the positive results of direct detection experiments (the annual modulation observed by DAMA ([Bernabei et al. 2008, 2010](#)) and CoGeNT ([Aalseth et al. 2011a,b](#)), and the hints of an observed excess of events on CRESST ([Angloher et al. 2012](#)) and CDMS-Si ([Agnese et al. 2013a,b](#))), and the constraints coming from null results (e.g. CDMS-Ge ([Ahmed et al. 2010](#)), XENON100 ([Aprile et al. 2011](#)) and very recently LUX ([Akerib et al. 2013](#))). The phenomenology of long-range DM-nucleus interactions in direct DM searches has been studied in Refs. ([Foot 2004a, 2008, 2010, 2012](#); [Fornengo et al. 2011](#); [Panci 2012](#)).

In this paper, we investigate how a DM-baryon Long Range Interaction (DMLRI), induced by the kinetic mixing of a new $U(1)$ gauge boson and the photon, affects the evolution of the Sun. The results obtained are then confronted with helioseismology data. The helioseismic data that we use was obtained by several international collaborations, such as the Solar and Heliospheric Observatory (SOHO) mission and the Birmingham Solar Oscillations Network (BiSON) observational network ([Turck-Chieze et al. 1997](#); [Basu et al. 2009](#)). Furthermore, we also discuss the constraints on the main parameters of long-range DM particle interactions which can be obtained from direct DM search data.

2. PROPERTIES OF DM WITH LONG-RANGE INTERACTIONS

In most of the classical models, one often assumes a symmetric dark sector in which the DM scattering off of baryon nuclei is done by a contact-like interaction. In our study, we will instead focus on a class of asymmetric DM

models in which the interaction between DM particles and target nuclei is mediated by a light messenger. If the typical momenta exchanged in the scattering is bigger than the mass of the mediator, a long-range interaction then arises.

A specific realization of this kind of picture is offered by particle physics models where a new $U(1)$ hidden gauge boson ϕ (dark photon) possesses a small kinetic mixing ϵ_ϕ with the photon. In this case, the interaction between a nucleus with mass m_T and electric charge Ze (Z is the number of protons in the baryon nucleus and e the electrical charge) and a DM particle with mass m_χ and dark charge $Z_\chi g_\chi$ (Z_χ and g_χ are the equivalent quantities of Z and e in the dark sector) is described in the non-relativistic limit by the following Yukawa potential (see e.g. [Feng et al. 2010](#); [Fornengo et al. 2011](#)),

$$V(r) = \epsilon_\phi k_\chi \frac{Z\alpha}{r} e^{-m_\phi r}, \quad (1)$$

where $\alpha = e^2/4\pi$ is the electromagnetic fine structure constant and the parameter $k_\chi = Z_\chi g_\chi/e$ measures the strength of the DM-dark photon coupling. Here m_ϕ is the mass of the dark photon that acts like an electronic cloud which screens the charges of the particles involved in the scattering. Since both k_χ and ϵ_ϕ are unknown, we define $\gamma_\phi \equiv k_\chi \epsilon_\phi$ and we treat it as a free parameter of our model together with m_χ and m_ϕ .

The differential cross section, neglecting the form factor of the target nuclei⁹, can be simply obtained by performing the Fourier transform of Eq. 1 and it reads

$$\frac{d\sigma_T}{d\Omega} = \frac{\xi_\chi^2 \mu^2}{(q^2 + m_\phi^2)^2}, \quad (2)$$

where $\xi_\chi = 2\alpha Z \gamma_\phi$, $\mu = m_\chi m_T / (m_\chi + m_T)$ is the DM-nucleus reduced mass and $q = \sqrt{2m_T E_R}$ is the momenta exchanged in the interaction with E_R the recoil energy. As is apparent from the dependence on the dark photon mass, two different regimes clearly appear:

- ◇ *Point-like limit* ($q \ll m_\phi$): In this regime the interaction is of a contact type. Indeed the differential cross section turns out to be proportional to ξ_χ^2/m_ϕ^4 which plays the same role as Fermi's constant in weak interactions. The interaction reduces to the “standard” spin-independent picture, apart from the fact that in this case, DM particles only couple with protons ($d\sigma_T/d\Omega \propto Z^2$).
- ◇ *Long-range limit* ($q \gg m_\phi$): In this regime, the differential cross section acquires an explicit dependence on the momenta exchanged in the interaction and therefore a Rutherford-like cross section arises ($d\sigma_T/d\Omega \propto 1/q^4$). This is extremely interesting because ideal experiments with very low energy threshold and light target nuclei (e.g. the Sun) are in principle more sensitive than the ones with high threshold and heavy targets (e.g. XENON100 and

⁹ The Sun being mostly composed of hydrogen and helium, we can justify neglecting the nuclear responses. On the other hand for the derivation of the direct detection constraints, we use the form factors provided in ref. ([Fitzpatrick et al. 2012](#)).

LUX). To give a concrete example, once DM particles are thermalized with baryons in the center of the Sun, their collisions occur with $q \simeq 1$ MeV considering a DM mass of 10 GeV. For direct detection experiments, the typical momenta transferred in the scattering is instead bigger ($q \gtrsim 20$ MeV). Thanks to this fact, we expect that DM models feature a long-range interaction with ordinary matter can affect the sound-speed radial profile of the Sun without being excluded by terrestrial experiments.

Having the differential cross section at our disposal, the key ingredient that sets the normalization of both the capture rate and the transport of energy by DM particles in the Sun is the energy transfer cross section. In the Born approximation, it reads,

$$\sigma_T(v_{\text{rel}}) = \frac{2\pi\beta_\phi^2}{m_\phi^2} \left[\ln(1 + r_\phi^2) - \frac{r_\phi^2}{1 + r_\phi^2} \right], \quad (3)$$

where $\beta_\phi = \xi_\chi m_\phi / (2\mu v_{\text{rel}})$, $r_\phi = 2\mu v_{\text{rel}} / m_\phi$, and v_{rel} is the relative velocity between the DM flux and the Sun. Unlike the customary DM models, in this case σ_T depends on v_{rel} in the long-range regime. Thanks to this main novelty, one therefore expects that the typical scattering cross section in the capture process differs compared to the one entering in the transport mechanism. On a more specific level, one has:

- ◊ *Capture:* In general, the infalling DM particles reach a given shell of radius r with a velocity $w(r) = \sqrt{v_0^2 + v_{\text{esc}}^2(r)}$. Here v_0 is the local DM dispersion velocity in our Galaxy and $v_{\text{esc}}(r)$ is the Sun's escape velocity at r . Since w is much larger than the thermal velocity, we assume that the relative velocity $v_{\text{rel}} \equiv w(r)$. Furthermore, since the total number of DM particles captured by the Sun is independent on r , it is a good approximation to define an average infalling DM velocity by

$$\bar{w} = 1/M_\odot \int d^3r w(r) \rho(r). \quad (4)$$

Here $\rho(r)$ is the Sun's mass density and $M_\odot = \int d^3r \rho(r)$ is its total mass. For instance, considering a typical velocity dispersion $v_0 = 220$ km/s, we get $\bar{w} \simeq 1120$ km/s. As explained in more detail in the next section, the capture rate is then computed numerically considering a constant cross section $\sigma_T^{\text{cap}} = \sigma_T(\bar{w})$.

- ◊ *Transport:* In this case, the typical relative velocity for the scattering is much smaller than \bar{w} being due to DM particles thermalized together with the ordinary plasma in the center of the Sun. It is then a good approximation to assume $v_{\text{rel}} \equiv v_{\text{th}}$, where $v_{\text{th}} = \sqrt{2T_c/m_\chi}$ is the thermal speed and T_c is the time-dependent temperature in the Sun's core. As explained in more detail in the next section, we compute the transport of energy numerically by considering $\sigma_T^{\text{tra}} = \sigma_T(v_{\text{th}})$. It is worth stressing that since the solar code follows the time evolution of the Sun, in the early stages the energy transport, and in turn the thermal conduction by DM particles, was much more efficient with T_c at

that time being smaller than the present-day central temperature.

In this study, we focus on the interaction of DM with hydrogen – the most abundant chemical element in the Sun's interior. Fig. 1 shows an illustrative example of the DM-hydrogen energy transfer cross section σ_T as a function of the mass of the dark photon m_ϕ for a fixed value of the kinetic mixing parameter $\gamma_\phi = 10^{-9}$ and a DM mass $m_\chi = 10$ GeV. On a more specific level we show in blue the scattering cross section responsible for the capture process σ_T^{cap} , while in red is shown the one entering into the energy transport mechanism σ_T^{tra} computed at the present time ($T_c^0 = 1.57 \times 10^7$ K). We can see that if the mass of the dark photon is smaller than a few MeV (long-range regime), the capture and the transport processes are controlled by different scattering cross sections. It is worth pointing out that in this limit, the ratio $\sigma_T^{\text{tra}}/\sigma_T^{\text{cap}}$ is barely dependent on m_ϕ , if m_χ is larger than the hydrogen mass. It instead depends on the mass of the DM particle through the thermal velocity relation and in particular for a 10 GeV candidate, $\sigma_T^{\text{tra}} \sim 10^3 \sigma_T^{\text{cap}}$. The main new aspect is actually given by this enhanced conduction in the inner part of the Sun compared to the usual DM models. Thanks indeed to this fact, DM particles, interacting via long-range forces with ordinary matter, can produce an impact on the helioseismology data without evading the constraints coming from direct DM search experiments.

In our analysis, we consider the observed sound speed radial profile of the Sun and compare it to the theoretical prediction over a broad range of DM masses ($4 \text{ GeV} \leq m_\chi \leq 20 \text{ GeV}$), dark photon masses ($0.1 \text{ keV} \leq m_\phi \leq 1 \text{ GeV}$) and kinetic mixing parameters ($10^{-12} \leq \gamma_\phi \leq 10^{-6}$). With these choices, the scattering cross-section spans a large interval of values from $5 \times 10^{-29} \text{ cm}^2$ to $8 \times 10^{-55} \text{ cm}^2$. The cross-section range of interest for the Sun corresponds to the values for which σ_T is close to the Sun's characteristic scattering cross-section, $\sigma_\star = m_p/M_\star R_\star^2$ where M_\star and R_\star are the mass and radius of the star. From the zero-age mean-sequence (ZAMS) until the present age of the Sun (4.6 Gyear), σ_\star takes values between $2.5 \times 10^{-32} \text{ cm}^2$ and $4 \times 10^{-36} \text{ cm}^2$.

3. DARK MATTER AND THE SUN

The Sun, as are all stars in the Milky Way, is immersed in a halo of DM. As with any other star in the galaxy, the Sun captures substantial numbers of DM particles during its evolution, but any impact on the star depends on the properties of these particles, as well as on the stellar dynamics and structure of the star. In general, for low-mass stars evolving in low density DM halos, the presence of DM inside the star changes its evolution by providing the star with a new mechanism to evacuate the heat produced in the stellar core (e.g., Lopes et al. 2002; Lopes & Silk 2002; Zentner & Hearin 2011; Lopes & Silk 2012a; Casanellas & Lopes 2013). This is quite different for stars evolving in DM halos of high density – as occurs during the formation of the first generation of stars. In these cases, the annihilation of DM particles supplies the star with an additional source of energy capable of substantially extending the lifetimes of

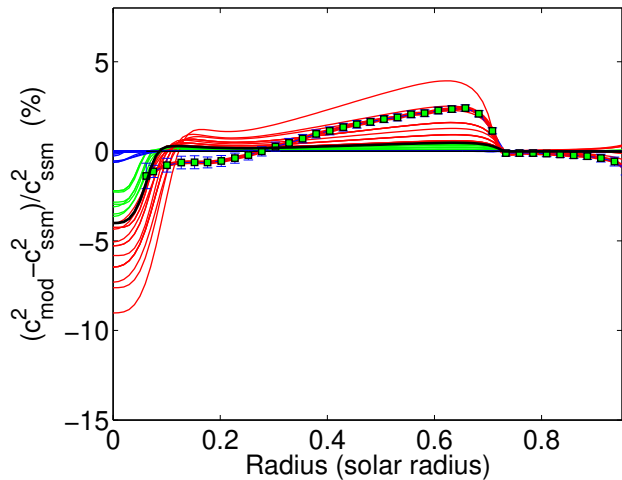


Figure 2. Comparison between the SSM sound speed radial profile c_{ssm}^2 (Lopes & Turck-Chieze 2013), the observed sound speed profile c_{obs}^2 (Turck-Chieze et al. 1997; Basu et al. 2009) and the sound speed of different DMLRI solar models c_{mod}^2 in which the DM particle and the mediator have masses in the followings intervals: $5 \text{ GeV} \leq m_\chi \leq 20 \text{ GeV}$, $0.1 \text{ keV} \leq m_\phi \leq 1 \text{ GeV}$, and coupling with baryons $\gamma_\phi = 10^{-9}$. The green-square dots correspond to the observed difference $\Delta c_{\text{obs}}^2 = (c_{\text{obs}}^2 - c_{\text{ssm}}^2)/c_{\text{ssm}}^2$, while the different continuous lines refer to $\Delta c^2 = (c_{\text{mod}}^2 - c_{\text{ssm}}^2)/c_{\text{ssm}}^2$. The DMLRI solar models were assembled accordingly to their impact in the Sun’s center: $\Delta c^2 < 2.0\%$ (blue curve), $2.0 < \Delta c^2 < 4.0\%$ (green curve) and $\Delta c^2 > 4.0\%$ (red curve). For example, the black line corresponds to an illustrative DMLRI model with benchmark parameters: $m_\chi = 10 \text{ GeV}$ and $m_\phi = 10 \text{ keV}$. Note: The observational error in $c_{\text{obs}} \pm \Delta c_{\text{obs}}$ is multiplied by a factor 10.

these stars (Scott et al. 2009; Casanellas & Lopes 2009; Lopes et al. 2011; Scott et al. 2011).

The computation of the impact of DM in the evolution of the Sun is done by a modified version of the CESAM code (Morel 1997; Morel & Lebreton 2008), which has been widely used to compute the SSM and for modelling other stars by different research groups (Deheuvels et al. 2010; Turck-Chieze et al. 2010; Lopes 2013; Lopes & Turck-Chieze 2013). In this study, we follow a procedure identical to other studies published in the literature by some of us as well as other authors (e.g., Lopes et al. 2002; Lopes & Silk 2002; Cumberbatch et al. 2010; Taoso et al. 2010; Lopes & Silk 2010a,b; Hamerly & Kosovichev 2012; Lopes & Silk 2012a,b; Lopes et al. 2014). Nevertheless, there are some important differences between this study and the previous ones, which we will highlight in the remainder of this section.

As commented upon in the previous section, the impact of DM in the Sun’s interior depends on two major physical processes: the accumulation of DM inside the star, and the efficiency of DM in transferring energy from the core to the external layers. In any case, the density of DM in the halo is the single major ingredient affecting the impact of DM in the Sun. As usually done in these studies, we consider that the local density of DM is $\rho_\odot = 0.38 \text{ GeV/cm}^3$ (Gates et al. 1995, 1996; Catena & Ullio 2010; Salucci et al. 2010). The choice of this value is in part made to facilitate the comparison with other work. Still, this is a very reliable value: the most recent estimates of ρ_\odot made by two independent groups have ob-

tained values of 0.3 GeV/cm^3 (Bovy & Tremaine 2012) and 0.85 GeV/cm^3 (Garbari et al. 2012). In particular (Garbari et al. 2012) argue that their new method is quite robust, and they have obtained their value at 90% confidence level. In our computation, we will also consider that the DM particles in the solar neighborhood have dispersion velocity $v_0 = 220 \text{ km/s}$ (see e.g., Bertone et al. 2005).

The accumulation of DM in the Sun’s core during its evolution from the beginning of the ZAMS until the present age (4.6 Gyear) is regulated by three physical processes: capture, annihilation and evaporation of DM particles. At each step of the evolution, the total number of DM particles N , that is captured by the star is given by

$$\frac{dN(t)}{dt} = \Gamma_{\text{cap}} - \Gamma_{\text{ann}}N(t)^2 - \Gamma_{\text{eva}}N(t), \quad (5)$$

where Γ_{cap} , Γ_{ann} and Γ_{eva} are the DM coefficients of capture, annihilation and evaporation rates. It is worth noticing that, unlike previous studies, in this work we resolve numerically the equation (5) for each step of the star’s evolution. A detailed discussion about these processes can be found in the literature (e.g., Griest & Seckel 1987; Lopes et al. 2011).

The capture rate Γ_{cap} is computed numerically from the expression obtained by Gould (1987) as implemented by Gondolo et al. (2004). The scattering of DM particles with the baryons inside the Sun is the main factor affecting the capture rate Γ_{cap} . We restrict our study to the scattering of DM particles to the most abundant element, i.e., hydrogen. We consider that the capture rate is controlled by σ_T^{cap} obtained by substituting v_{rel} with the averaged infalling speed \bar{w} in Eq. (3) as briefly explained in the previous section. In particular, in the long-range regime ($r_\phi \gg 1$ or in terms of the exchanged momenta, $q \gg m_\phi$), the DM-hydrogen energy transfer cross section responsible for the capture process is independent of m_χ and logarithmically dependent on m_ϕ . It reads

$$\lim_{r_\phi \gg 1} \sigma_T^{\text{cap}} = 4\pi \frac{\alpha^2 \gamma_\phi^2}{m_p^2 \bar{w}^4} L_\phi^{\text{cap}}(m_\phi) \simeq \left(\frac{\gamma_\phi}{10^{-9}}\right)^2 \left(\frac{L_\phi^{\text{cap}}}{L_\phi^{\text{cap}}}\right) \cdot 9.9 \times 10^{-39} \text{ cm}^2, \quad (6)$$

where $L_\phi^{\text{cap}} = \ln(2m_p \bar{w}/m_\phi)$ is a sort of Coulomb logarithm that measures the strength of the screening effect in the capture process and $L_\phi^{\text{cap}} \simeq 6.6$ is its value for $m_\phi = 10 \text{ keV}$.

The other chemical elements are underabundant, consequently their contribution for the capture of DM is negligible. The dependence of the scattering cross-section on the parameter space of long-range DM particles is given by equation (3). The description of how this capture process is implemented in our code is discussed in Lopes et al. (2011).

Since we assume a primordial asymmetry between particles and anti-particles in the dark sector, the annihilation rate Γ_{ann} is set to be zero. This is justified by the fact that the DM asymmetry (analogous to the baryon

asymmetry) guarantees an over-abundance of particles relative to antiparticles in the present day Universe.

The evaporation rate Γ_{eva} is relevant only for very light particles, i.e., particles with $m_\chi \leq 4$ GeV (Gould 1990). Kappl & Winkler (2011) estimated the evaporation mass for DM particles in the Sun, m_{eva} , to be such that $m_{\text{eva}} = 3.02 + 0.32 \log_{10}(\sigma_T/10^{-40} \text{cm}^2)$ GeV. If $m_\chi \leq m_{\text{eva}}$ the DM particle escapes the solar gravitational field and consequently has no impact on the structure of the star. Kappl & Winkler (2011) also found that the evaporation of DM particles is completely irrelevant for $m \geq 8$ GeV. It is worth noticing the fact that because the evaporation boundary has an exponential dependency on the mass and the scattering cross-section of the DM particle (Gould 1990), it follows that if m_χ exceeds m_{eva} by a few percent, then the evaporation of DM particles is totally negligible. Furthermore it is also important to point out that our DM model can easily have a quite large self-interaction in the long-range regime with size similar to the electromagnetic scattering. If then this self-interaction is attractive (e.g. this can be obtained if the dark sector is composed by light and heavy species with a different sign of the dark charge $Z_\chi g_\chi$) we expect that Γ_{eva} can be set to zero for DM masses below 4 GeV as well, in such cases the properties of the dark plasma being similar to the ordinary one (electrons are indeed trapped in the Sun). We leave further discussion of this important effect for future studies.

In our computation, we use Γ_{eva} estimated by Busoni et al. (2013) in the regime where the Sun is optically thin with respect to the DM particles. Nevertheless, we restrict our analysis to particles with mass larger than 4 GeV, for which the evaporation rate is almost negligible.

Once gravitationally captured by the star, the DM particles thermalise with baryons after a few Kepler orbits around the solar centre, colliding through elastic scattering with hydrogen and other elements, and thus providing the star with an alternative mechanism for the transport of energy. The relatively efficiency of the DM energy transport in relation to the radiative heat transport depends on the Knudsen number, $K_\chi = l_\chi/r_\chi$ where l_χ is the free mean path of the DM particle inside the star and r_χ is the characteristic radius of the DM distribution (Gilliland et al. 1986; Lopes et al. 2002). Depending on the value of σ_T , the transport of energy by DM is local (conductive) or non-local, which corresponds to $K_\chi \ll 1$ or $K_\chi \gg 1$. We assume that the thermal conduction by DM particles is controlled by σ_T^{tra} obtained by substituting v_{rel} with the thermal speed v_{th} in Eq. (3) as briefly explained in the previous section. Unlike the cross section responsible for the capture process, in the long-range limit σ_T^{tra} depends on the DM mass via the thermal velocity v_{th} . It explicitly reads

$$\lim_{r_\phi \gg 1} \sigma_T^{\text{tra}} = \pi \frac{\alpha^2 \gamma_\phi^2 m_\chi^2}{m_p^2 T_c^2} L_\phi^{\text{tra}}(m_\chi, m_\phi, T_c) \simeq \left(\frac{m_\chi}{10 \text{ GeV}}\right)^2 \left(\frac{T_c}{T_c^0}\right)^2 \left(\frac{\gamma_\phi}{10^{-9}}\right)^2 \left(\frac{L_\phi^{\text{tra}}}{L_\phi^{\text{tra}_0}}\right) \cdot 1.9 \times 10^{-35} \text{ cm}^2, \quad (7)$$

where $L_\phi^{\text{tra}}(m_\chi, m_\phi, T_c) = 1/2 \ln(8m_p^2 T_c / (m_\chi m_\phi^2))$ em-

ulates the screening effect in the energy transport and $\bar{L}_\phi^{\text{tra}} \simeq 4.6$ is its value for $m_\phi = 10$ keV, $m_\chi = 10$ GeV and $T_c = T_c^0$. Depending on the free parameters of the model scanned in our analysis, the energy transfer cross section covers a broad range of values ($5 \times 10^{-29} \text{ cm}^2 \leq \sigma_T^{\text{tra}} \leq 8 \times 10^{-55} \text{ cm}^2$). In this case the corresponding range of the Knudsen number is ($5 \times 10^{-9} \leq K_\chi \leq 3 \times 10^{18}$). Both mechanisms of energy transport are considered in this study (Gilliland et al. 1986; Lopes et al. 2002). In the case of the non-local regime, we follow the numerical prescription of Gould & Raffelt (1990) rather than the original one proposed by Spergel & Press (1985).

We note that in the long-range limit, the conduction is mainly local due to the fact that a Rutherford-like DM-baryon interaction can significantly enhance the energy transport ($\sigma_T^{\text{tra}} \gg \sigma_T^{\text{cap}}$) compared to the usual picture (indeed for the standard spin-independent and spin-dependent cases, one always has $\sigma_T^{\text{tra}} = \sigma_T^{\text{cap}}$). This is the main new element, and in particular, as we will see in Sec. 5, this class of models with enhanced energy transport can solve the so-called solar abundance problem without being excluded by direct searches experiments.

A similar conclusion can also be found in Ref. (Vincent & Scott 2013). In particular they implement the formalism of Gould & Raffelt (1990) in order to properly account for both velocity and exchanged momenta dependencies in the differential cross section. Although their method is more refined compare to the one we are using they did not incorporate their results in a solar simulation software yet.

4. DISCUSSION

The impact of DM in the Sun is studied by inferring the modifications that DM causes to the Sun's structure and to the solar observables. In the following, the standard solar model (SSM; e.g., Turck-Chieze & Lopes 1993; Lopes 2013) is used as our model of reference, which predicts solar neutrino fluxes and helioseismology data consistent with current measurements. The excellent agreement obtained between theory and observation results from the combined effort between the fields of helioseismology and solar modelling, a collaboration extended by several decades which lead to a high precision description of physical processes present inside the Sun (Turck-Chieze & Couvidat 2011; Turck-Chieze & Lopes 2012). This was very relevant in the case of the physical processes related with microscopic physics, including the equation of state, opacities, nuclear reactions rates, and microscopic diffusion of helium and heavy elements. A detailed discussion about current predictions of the SSM and their uncertainties can be found in the literature (e.g., Turck-Chieze & Lopes 1993; Serenelli et al. 2009; Guzik & Mussack 2010; Turck-Chieze et al. 2010; Lopes & Turck-Chieze 2013; Lopes 2013; Lopes & Silk 2013).

In Fig. 2 the green square dots show the difference between the square of the sound speed profile c_{ssm}^2 obtained from the SSM and the square sound speed profile c_{obs}^2 computed by an inversion technique from helioseismol-

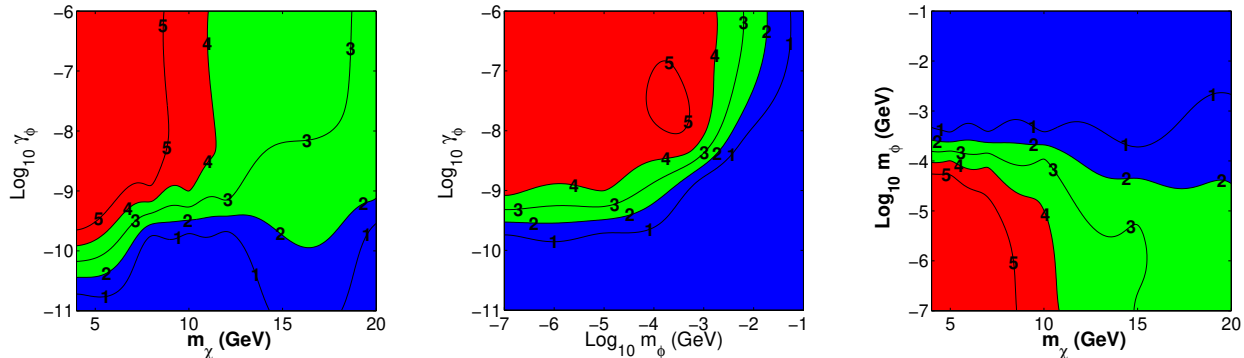


Figure 3. The maximum sound speed difference $\Delta c_{\max}^2 = \max[(c_{\text{mod}}^2 - c_{\text{SSM}}^2)/c_{\text{SSM}}^2]$ in the full parameter space of DMLRI models $(\gamma_\phi, m_\chi, m_\phi)$. *Left panel:* Parameter space projected in the (m_χ, γ_ϕ) plane keeping fix $m_\phi = 10$ keV; *Central panel:* Parameter space in the (m_ϕ, γ_ϕ) plane considering $m_\chi = 10$ GeV; *Right panel:* Projection of the parameter space in the (m_χ, m_ϕ) plane for a fix $\gamma_\phi = 10^{-9}$. In all panels the red(blue) areas individuate the regions of the parameter space where $\Delta c_{\max}^2 > 4\%$ ($\Delta c_{\max}^2 < 2\%$) while those in light green refer to the regions where the agreement with helioseismic data is better than the SSM ($2\% < \Delta c_{\max}^2 < 4\%$). All the DMLRI models in the red regions are excluded since they produce a large impact on the Sun’s core sound speed profile. The DM halo in the Galaxy has been assumed in the form of an isothermal sphere with local energy density $\rho_\odot = 0.38$ GeV/cm³ and velocity dispersion $v_0 = 220$ km/s.

ogy data (Turck-Chieze et al. 1997; Basu et al. 2009). The relative sound speed difference $(c_{\text{obs}}^2 - c_{\text{SSM}}^2)/c_{\text{SSM}}^2$ is smaller than 2% throughout the interior of the Sun. Nevertheless, it is important to observe that in the very center of the Sun (for $r \leq 0.2 R_\odot$) the seismology data available for the sound speed inversion is quite sparse. Although, the error-bars of c_{obs}^2 are quite small (cf. Fig. 2), the sound speed inversion in this region is not fully reliable. Accordingly, we choose to consider that the uncertainty is of the order of 4% rather than 2%. In the remainder of the article we will refer to this value as the *SSM uncertainty*, meaning the uncertainty related to the physical processes of the SSM and helioseismology sound speed inversion.

The DMLRI solar models were obtained in an identical manner to the SSM, by adjusting the initial helium Y_i and the mixing length parameter α_{MLT} in such a way that at the present age (4.6 Gyear), these solar models reproduced the observed values of the mass, radius and luminosity of the Sun, as well as the observed photospheric abundance ratio $(Z/X)_\odot$, where X and Z are the mass fraction of hydrogen and the mass fraction of elements heavier than helium, respectively. In Fig. 2 the different continuous lines show the squared sound speed difference $\Delta c^2 = (c_{\text{mod}}^2 - c_{\text{SSM}}^2)/c_{\text{SSM}}^2$, where c_{mod} is the sound speed of the DMLRI solar model. These solar models are obtained for a reference value of $\gamma_\phi = 10^{-9}$ and different values of m_χ and m_ϕ .

The DM impact is most visible in the core of the star where the DM particles accumulate, however, because the solar models are required to have the current observed values of radius and luminosity, a decrease of the production of nuclear energy in the Sun’s core due to the reduction of the central temperature (caused by the thermalisation of DM with baryons), is compensated by an increase of the sound speed in the radiative region. As shown in Fig. 2 all the DMLRI solar models have an identical impact behaviour on the solar structure, however, based upon the parameters m_χ and m_ϕ it is possible to distinguish three sets of models: *i*) DMLRI models for which the squared sound speed difference is larger than the *SSM uncertainty* (red curves); *ii*) DMLRI models for

which the agreement with the helioseismic data is better than the current SSM (green curves); *iii*) DMLRI models for which the squared sound speed difference is smaller than the *SSM uncertainty* (blue curves). As an example in Fig. 2 we also shown an illustrative DMGRI solar model with benchmark parameters: $m_\chi = 10$ GeV, $m_\phi = 10$ keV and $\gamma_\phi = 10^{-9}$ (black curve).

Fig. 3 shows the maximum sound speed difference $\Delta c_{\max}^2 = \max[(c_{\text{mod}}^2 - c_{\text{SSM}}^2)/c_{\text{SSM}}^2]$ in the full parameter space of DMLRI models $(\gamma_\phi, m_\chi, m_\phi)$. The represented percentages are performed for $r \leq 0.3 R_\odot$. On a more specific level in the right panel of Fig. 3 we project the parameter space in the (m_χ, γ_ϕ) plane by choosing $m_\phi = 10$ keV. In the central plane the (m_ϕ, γ_ϕ) plane is shown for $m_\chi = 10$ GeV, while on the left panel, the parameter space is projected in the (m_χ, m_ϕ) plane keeping fix $\gamma_\phi = 10^{-9}$. Once Δc_{\max}^2 is larger than the *SSM uncertainty* it is reasonable to exclude all DMLRI models, since they produce a large impact on the Sun’s core sound speed profile (red regions). On the other hand, if Δc_{\max}^2 is in the range 2% – 4% the agreement with the helioseismic data, as commented upon above, is improved (green regions). For instance, we find that DM particles with a mass in the range 4 GeV–8.5 GeV coupled with ordinary baryons via a kinetic mixing parameter γ_ϕ bigger than 10^{-9} , produce a very large impact on the Sun’s core in the long-range regime (m_ϕ smaller than a few MeV). Therefore they can be excluded as possible DM candidates. On the other hand, we can see that DM particles with a mass of the order of 10 GeV, a kinetic mixing parameter in the range $(3 \times 10^{-10} - 10^{-9})$ and a mediator with a mass smaller than a few MeV improve the agreement between the best solar model and the helioseismic data. This is quite interesting since direct DM searches experiments, as we shall see in the next section, either do not, or barely exclude, these kinds of DM models with long-range interactions with baryons.

5. COMPLEMENTARY CONSTRAINTS

In this section, we present the complementary constraints which are relevant for DMLRI models. A first class of them come from terrestrial direct detection experiments. In particular, since the interactions consid-

ered in our work is spin-independent, we only compute the constraints coming from the XENON100 and LUX experiments. The details on the experimental results and the statistical analysis used to treat the datasets can be found in (Cirelli et al. 2013). In Fig. 4 we show the constraints in the relevant parameter spaces of our model. As we did in the previous section, we project the parameter space in the (m_χ, γ_ϕ) plane (left panel), (m_ϕ, γ_ϕ) plane (central panel) and (m_χ, m_ϕ) plane (right panel). The dark blue (red) lines refer to the constraints coming from XENON100(LUX), while the different hatching (dotted, dashed-dotted, dashed) indicates the three values of the third direction in the parameter space that we kept fixed ($m_\phi = (1, 0.1, \leq 0.01)$ GeV on the left panel, $m_\chi = (6, 10, 14)$ GeV on the central panel and $\gamma_\phi = (10^{-8}, 10^{-9}, 10^{-9.5})$ on the right panel). The areas of the parameter space above the first and second plots, and the ones below the third plot are excluded. Similar constraints can also be found in Ref. (Kaplinghat et al. 2013). We can see that in the long-range regime (mediator masses below roughly 10 MeV), the constraints becomes independent of m_ϕ . Indeed in this case, the interaction is Rutherford-like and therefore the differential cross section in Eq. (2), which sets the normalization of the total number of events in certain experiments, solely depends on the exchanged momentum q . By virtue of this fact, we can just use the left plot of Fig. 4 and compare it directly with the results shown in Fig. 3. We can see that in the relevant DM mass range that affects helioseismic data (4–20) GeV, the constraints, coming from the LUX experiments, exclude DMLRI models that are coupled with baryons through kinetic mixing parameters larger than roughly $(2 \times 10^{-7}, 2 \times 10^{-10})$. Therefore, as is apparent, long-range spin-independent DM-baryon interactions can easily improve the agreement between the best solar model and the helioseismic data without being excluded by direct detection experiments for a broad range of DM masses. Indeed, as we have already pointed out, the Sun is an ideal experiments for DM models which posses an enhanced cross section with baryons for small momentum exchanges.

A second class of complementary constraints that only depends on the properties of the dark photon (kinetic mixing parameter ϵ_ϕ and its mass m_ϕ) are those coming from supernovæ observations and beam dump neutrino experiments. These are presented, for instance, in the (m_ϕ, ϵ_ϕ) plane in Fig. 6 of (Essig et al. 2013). We can see that the most stringent constraint comes from supernova observations (namely the energy loss observed from SN1987a): it indeed constrains relatively small kinetic mixing parameters (ϵ_ϕ above roughly 10^{-10}) and light messengers (m_ϕ below 1 MeV). Nevertheless since, as already stated, the normalization of the energy transfer cross-section σ_T depends not only on the properties of the dark photon but on its coupling with the DM particles measured by the parameter k_χ as well, the bounds can be relaxed if a larger coupling is taken into account. For example, if $k_\chi = 10$, the constraint on γ_ϕ can be obtained by shifting the one on ϵ_ϕ of the same factor up. It is worth pointing out that such large values of k_χ can be simply achieved either in models of composite DM with large Z_χ (e.g. mirror models) or in those with a strongly coupled dark sector ($g_\chi > e$). Furthermore it is

also relevant to stress that for pure long-range interactions ($m_\phi = 0$), most of the constraints commented upon above do not apply at all, the direct production of dark photons being forbidden for kinematical reasons (see e.g. Fig. 7 in Ref. (Essig et al. 2013)).

A third class of constraints which instead solely depend on the characteristics on the dark sector itself are those coming from self-interactions. Indeed, since for this type of model, the DM-DM scattering is not suppressed by ϵ_ϕ , the self-interactions, especially in the long-range limit, can easily reach large values, affecting the dynamics of virialized astrophysical objects. In Refs. (Tulin et al. 2013; Kaplinghat et al. 2013), the constraints on m_ϕ coming from the observations of a few elliptical DM halos have been presented. These constraints are in general very stringent for DM masses below 10 GeV: in this case, in fact, the time over which energy is transferred in the system is extremely rapid and therefore a spherical DM halo tends to form in contradiction with observations. In particular, dark photon masses below roughly 100 MeV are excluded. However, the derivation of this last class of constraints is very uncertain, both from the theoretical and experimental side, because we do not really know how virialized astrophysical objects are formed in the presence of a DM sector with long-range interactions. Indeed, since the self-interaction needed to change their dynamics is in general of the order of the Thompson scattering ($\sigma_{em} \simeq 10^{-24}$ cm²), from trivial dimensional analysis of such large cross sections, the following rough estimate yields that the self-interaction is of a long-range type in most of the virialized astrophysical objects under the assumption that the DM-dark photon coupling is of the order of α . In this case, the probability to radiate a dark photon in the scattering process is different from zero and therefore it might well be possible that the DM sector is dissipative just like our sector. The time over which energy is transferred in the system is no longer a good indicator, since the relevant quantity that describes the dynamical evolution of the system is now the cooling time: in particular, for a DM sector composed of heavy and light species, the dissipation time due to the soft emission of dark photons (dark bremsstrahlung) can be smaller than the age of the virialized astrophysical objects (see e.g. Fan et al. 2013a,b; McCullough & Randall 2013). In this case, the system is no longer stable and in general it starts to collapse. By virtue of this fact, we do not consider this last class of constraints, since a more dedicated and careful analysis also involving numerical simulations is clearly needed.

6. CONCLUSION AND SUMMARY

We have examined how DM-baryon long-range interactions can affect the Sun’s sound speed radial profile. The phenomenological approach used in our analysis lets us explore all the parameter space from the contact regime to the long-range regime. We find that DM particles lighter than 8.5 GeV coupled with ordinary baryons through a kinetic mixing parameter γ_ϕ bigger than 10^{-9} , produce a very large impact on the Sun’s core in the long-range regime (m_ϕ smaller than few MeV). Therefore they can be excluded as possible DM candidates. However, solar models for which the DM particle has a mass of 10 GeV and the mediator a mass smaller than

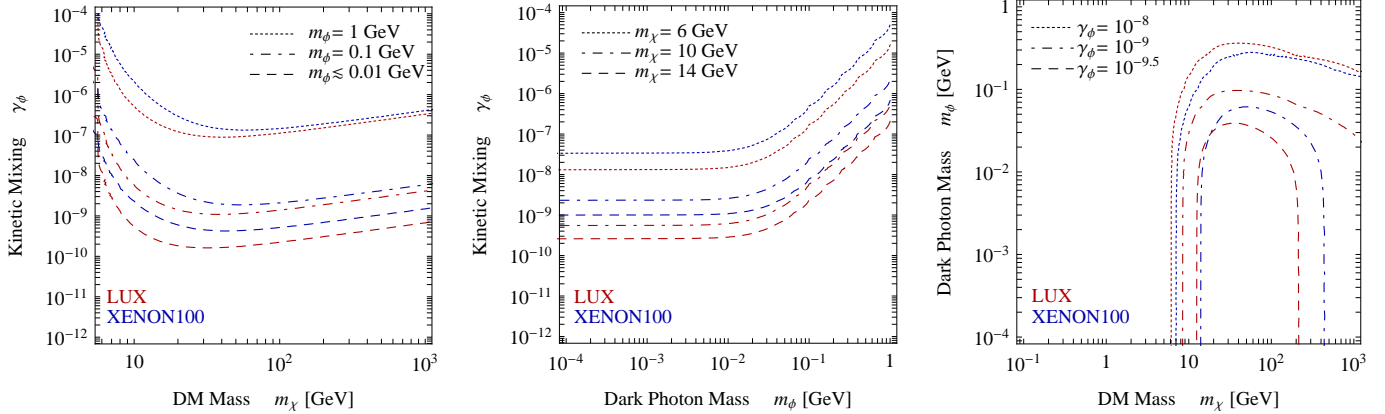


Figure 4. Direct detection constraints in the relevant parameter space of DMLRI models. *Left panel:* Parameter space projected in the (m_χ, γ_ϕ) plane; *Central panel:* Parameter space in the (m_ϕ, γ_ϕ) plane; *Right panel:* Projection of the parameter space in the (m_χ, m_ϕ) plane. In all panels, the dark blue (red) lines refer to the constraints coming from XENON100 (LUX), while the different hatching (dotted, dashed-dotted, dashed) indicates the three values of the third direction in the parameter space we kept fixed ($m_\phi = (1, 0.1, \leq 0.01)$ GeV on the left panel, $m_\chi = (6, 10, 14)$ GeV on the central panel and $\gamma_\phi = (10^{-8}, 10^{-9}, 10^{-9.5})$ on the right panel). Like in Fig. 3, the bounds are computed by assuming an isothermal halo with $\rho_\odot = 0.38$ GeV/cm³ and $v_0 = 220$ km/s.

1 MeV improve the agreement with helioseismic data. Nevertheless, when the mass of the dark photon is larger than 10 MeV the impact on the Sun’s structure is very small, being in this case the interaction of a contact-type (standard spin-independent picture). In particular, the results obtained here reveal that DM models featuring a long-range interaction with ordinary matter can affect the sound-speed radial profile and in turn probably solve the so-called solar abundance problem without being excluded by terrestrial experiments (e.g. LUX and XENON100) in which the scattering cross section is suppressed by the strong inverse dependence on q . The Sun is in fact an ideal DM detector for the type of particle considered here, since it measures the entire nuclear recoil energy spectra in the scatterings.

To summarize, in this work we have obtained two main results. Firstly, for the first time, a DM-baryon velocity dependent total cross-section has been implemented in solar simulation software. Secondly, but even more importantly, our analysis shows that DM particles with a mass of 10 GeV and a long-range interaction with ordinary matter mediated by a very light mediator (below roughly a few MeV), can have an impact on the Sun’s sound speed profile without violating the constraints coming from direct DM searches. Furthermore, as commented upon in Sec. 5, it might well be possible that a dark sector with long-range forces can dissipate a relevant amount of energy through the emission of dark photons. A dissipative dark sector is extremely interesting because it can offer a rich array of new ideas ranging from the detection of primordial dark radiation to new possibilities for DM dynamics in virialized astrophysical objects.

This work was supported by grants from “Fundação para a Ciência e Tecnologia” and “Fundação Calouste Gulbenkian”. This research has been supported at IAP by ERC project 267117 (DARK) hosted by Université Pierre et Marie Curie - Paris 6, and at JHU by NSF

grant OIA-1124403.

REFERENCES

- Aalseth, C., Barbeau, P., Colaresi, J., Collar, J., Diaz Leon, J., et al. 2011a, Phys.Rev.Lett., 107, 141301 [LINK]
Aalseth, C. et al. 2011b, Phys.Rev.Lett., 106, 131301 [LINK]
Ade, P. et al. 2013, arXiv.org, 1303.5076 [LINK]
Agnese, R. et al. 2013a, arXiv.org, 1304.4279 [LINK]
— 2013b, Phys.Rev., D88, 031104 [LINK]
Ahmed, Z. et al. 2010, Science, 327, 1619 [LINK]
Akerib, D. et al. 2013, arXiv.org, 1310.8214 [LINK]
Angloher, G., Bauer, M., Bavykina, I., Bento, A., Bucci, C., et al. 2012, Eur.Phys.J., C72, 1971 [LINK]
Aprile, E. et al. 2011, Phys.Rev.Lett., 107, 131302 [LINK]
Basu, S., Chaplin, W. J., Elsworth, Y., New, R., & Serenelli, A. M. 2009, Astrophys.J., 699, 1403 [LINK]
Bereziani, Z. 2005, arXiv.org, hep-ph/0508233 [LINK]
Bereziani, Z., Ciarcelluti, P., Comelli, D., & Villante, F. L. 2005, Int.J.Mod.Phys., D14, 107 [LINK]
Bereziani, Z., Comelli, D., & Villante, F. L. 2001, Phys.Lett., B503, 362 [LINK]
Bernabei, R. et al. 2008, Eur.Phys.J., C56, 333 [LINK]
— 2010, Eur.Phys.J., C67, 39 [LINK]
Bertone, G., Hooper, D., & Silk, J. 2005, Phys.Rept., 405, 279 [LINK]
Blinnikov, S. & Khlopov, M. Y. 1982, Sov.J.Nucl.Phys., 36, 472 [LINK]
— 1983, Sov.Astron., 27, 371 [LINK]
Bovy, J. & Tremaine, S. 2012, Astrophys.J., 756, 89 [LINK]
Busoni, G., De Simone, A., & Huang, W.-C. 2013, JCAP, 1307, 010 [LINK]
Casanelas, J. & Lopes, I. 2009, Astrophys.J., 705, 135 [LINK]
— 2013, Astrophys.J., 765, L21 [LINK]
Catena, R. & Ullio, P. 2010, JCAP, 08, 004 [LINK]
Cirelli, M., Del Nobile, E., & Panci, P. 2013, JCAP, 1310, 019 [LINK]
Cumberbatch, D. T., Guzik, J., Silk, J., Watson, L. S., & West, S. M. 2010, Phys.Rev., D82, 103503 [LINK]
de Blok, W. 2010, Adv.Astron., 2010, 789293 [LINK]
Deheuvels, S., Michel, E., Goupil, M., Marques, J., Mosser, B., et al. 2010, A & A, 514, 31 [LINK]
Essig, R., Jaros, J. A., Wester, W., Adrian, P. H., Andreas, S., et al. 2013, arXiv.org, 1311.0029 [LINK]
Fan, J., Katz, A., Randall, L., & Reece, M. 2013a, Phys.Rev.Lett., 110, 211302 [LINK]
— 2013b, Phys.Dark Univ., 2, 139 [LINK]
Feng, J. L., Kaplinghat, M., & Yu, H.-B. 2010, Phys.Rev.Lett., 104, 151301 [LINK]

- Fitzpatrick, A. L., Haxton, W., Katz, E., Lubbers, N., & Xu, Y. 2012, *JCAP*, 1302, 004 [\[LINK\]](#)
- Foot, R. 2004a, *Phys.Rev.*, D69, 36001 [\[LINK\]](#)
- 2004b, *Int.J.Mod.Phys.*, D13, 2161 [\[LINK\]](#)
- 2008, *Phys.Rev.*, D78, 043529 [\[LINK\]](#)
- 2010, *Phys.Lett.*, B692, 65 [\[LINK\]](#)
- 2012, *Phys.Rev.*, D86, 023524 [\[LINK\]](#)
- Fornengo, N., Panci, P., & Regis, M. 2011, *Phys.Rev.*, D84, 115002 [\[LINK\]](#)
- Garbari, S., Liu, C., Read, J. I., & Lake, G. 2012, *MNRAS*, 425, 1445 [\[LINK\]](#)
- Garrison-Kimmel, S., Rocha, M., Boylan-Kolchin, M., Bullock, J., & Lally. 2013, *MNRAS*, 433, 3539 [\[LINK\]](#)
- Gates, E. L., Gyuk, G., & Turner, M. S. 1995, *Astrophys.J.*, 449, L123 [\[LINK\]](#)
- 1996, *Phys.Rev.*, D53, 4138 [\[LINK\]](#)
- Gilliland, R. L., Faulkner, J., Press, W. H., & Spergel, D. N. 1986, *Astrophys.J.*, 306, 703 [\[LINK\]](#)
- Gondolo, P., Edsjo, J., Ullio, P., Bergstrom, L., Schelke, M., et al. 2004, *JCAP*, 0407, 008 [\[LINK\]](#)
- Gould, A. 1987, *Astrophys.J.*, 321, 571 [\[LINK\]](#)
- 1990, *Astrophys.J.*, 356, 302 [\[LINK\]](#)
- Gould, A. & Raffelt, G. 1990, *Astrophys.J.*, 352, 654 [\[LINK\]](#)
- Griest, K. & Seckel, D. 1987, *Nucl.Phys.*, B283, 681 [\[LINK\]](#)
- Guo, Q., White, S., Angulo, R. E., Henriques, B., Lemson, G., et al. 2013, *MNRAS*, 428, 1351 [\[LINK\]](#)
- Guzik, J. A. & Mussack, K. 2010, *Astrophys.J.*, 713, 1108 [\[LINK\]](#)
- Hamerly, R. & Kosovichev, A. G. 2012, *arXiv.org*, 1110.1169 [\[LINK\]](#)
- Hinshaw, G. et al. 2013, *Astrophys.J.Suppl.*, 208, 19 [\[LINK\]](#)
- Kaplinghat, M., Tulin, S., & Yu, H.-B. 2013, *arXiv.org*, 1310.7945 [\[LINK\]](#)
- Kappl, R. & Winkler, M. W. 2011, *Nucl.Phys.*, B850, 505 [\[LINK\]](#)
- Klypin, A. A., Kravtsov, A. V., Valenzuela, O., & Prada, F. 1999, *Astrophys.J.*, 522, 82 [\[LINK\]](#)
- Kobzarev, I., Okun, L., & Pomeranchuk, I. 1966, *Sov.J.Nucl.Phys.*, 3, 837
- Lee, T. & Yang, C.-N. 1956, *Phys.Rev.*, 104, 254 [\[LINK\]](#)
- Loeb, A. & Weiner, N. 2011, *Phys.Rev.Lett.*, 106, 171302 [\[LINK\]](#)
- Lopes, I. 2013, *Phys.Rev.*, D88, 045006 [\[LINK\]](#)
- Lopes, I., Casanellas, J., & Eugenio, D. 2011, *Phys.Rev.*, D83, 63521 [\[LINK\]](#)
- Lopes, I., Kadota, K. & Silk, J. 2014, *Astrophys.J.*, 722, L95 [\[LINK\]](#)
- Lopes, I. & Silk, J. 2002, *Phys.Rev.Lett.*, 88, 151303 [\[LINK\]](#)
- 2010a, *Science*, 330, 462 [\[LINK\]](#)
- 2010b, *Astrophys.J.*, 722, L95 [\[LINK\]](#)
- 2012a, *Astrophys.J.*, 757, 130 [\[LINK\]](#)
- 2012b, *Astrophys.J.*, 752, 129 [\[LINK\]](#)
- 2013, *MNRAS*, 435, 2109 [\[LINK\]](#)
- Lopes, I. & Turck-Chieze, S. 2013, *Astrophys.J.*, 765, 14 [\[LINK\]](#)
- Lopes, I. P., Silk, J., & Hansen, S. H. 2002, *MNRAS*, 331, 361 [\[LINK\]](#)
- McCullough, M. & Randall, L. 2013, *JCAP*, 1310, 058 [\[LINK\]](#)
- Morel, P. 1997, *A & A Supplement series*, 124, 597 [\[LINK\]](#)
- Morel, P. & Lebreton, Y. 2008, *Astrophys.Space Sci.*, 316, 61 [\[LINK\]](#)
- Navarro, J. F., Ludlow, A., Springel, V., Wang, J., Vogelsberger, M., et al. 2010, *MNRAS*, 402, 21 [\[LINK\]](#)
- Panci, P. 2012, *arXiv.org*, 1206.2240 [\[LINK\]](#)
- Petraki, K. & Volkas, R. R. 2013, *Int.J.Mod.Phys.*, A28, 1330028 [\[LINK\]](#)
- Rocha, M., Peter, A. H., Bullock, J. S., Kaplinghat, M., Garrison-Kimmel, S., et al. 2013, *MNRAS*, 430, 81 [\[LINK\]](#)
- Salucci, P., Nesti, F., Gentile, G., & Martins, C. 2010, *A & A*, 523, A83 [\[LINK\]](#)
- Scott, P., Fairbairn, M., & Edsjo, J. 2009, *MNRAS*, 394, 82 [\[LINK\]](#)
- Scott, P., Venkatesan, A., Roebber, E., Gondolo, P., Pierpaoli, E., et al. 2011, *Astrophys.J.*, 742, 129 [\[LINK\]](#)
- Serenelli, A., Basu, S., Ferguson, J. W., & Asplund, M. 2009, *Astrophys.J.*, 705, L123 [\[LINK\]](#)
- Spergel, D. & Press, W. 1985, *Astrophys.J.*, 294, 663 [\[LINK\]](#)
- Taoso, M., Iocco, F., Meynet, G., Bertone, G., & Eggenberger, P. 2010, *Phys.Rev.*, D82, 83509 [\[LINK\]](#)
- Tulin, S., Yu, H.-B., & Zurek, K. M. 2013, *Phys.Rev.*, D87, 115007 [\[LINK\]](#)
- Turck-Chieze, S., Basu, S., Brun, A. S., Christensen-Dalsgaard, J., Eff-Darwich, A., et al. 1997, *Solar Phys.*, 175, 247 [\[LINK\]](#)
- Turck-Chieze, S. & Couvidat, S. 2011, *Rept.Prog.Phys.*, 74, 086901 [\[LINK\]](#)
- Turck-Chieze, S. & Lopes, I. 1993, *Astrophys.J.*, 408, 347 [\[LINK\]](#)
- 2012, *Res.Astron.Astrophys.*, 12, 1107 [\[LINK\]](#)
- Turck-Chieze, S., Palacios, A., Marques, J., & Nghiem, P. 2010, *Astrophys.J.*, 715, 1539 [\[LINK\]](#)
- Vincent, A. C. & Scott, P. 2013, *arXiv.org*, 1311.2074 [\[LINK\]](#)
- Zentner, A. R. & Hearin, A. P. 2011, *Phys.Rev.*, D84, 101302 [\[LINK\]](#)